JAM-A as a potential surface marker of human pluripotent stem cells

Sarah A. Konze, Julia Beimdiek, Astrid Oberbeck, Falk F. R. Buettner

Angaben zur Veröffentlichung / Publication details:

Konze, Sarah A., Julia Beimdiek, Astrid Oberbeck, and Falk F. R. Buettner. 2026. "JAM-A as a potential surface marker of human pluripotent stem cells." *Journal of Proteomics* 330: 105680. https://doi.org/10.1016/j.jprot.2026.105680.

Journal of Proteomics 330 (2026) 105680

Contents lists available at ScienceDirect

Journal of Proteomics

journal homepage: www.elsevier.com/locate/jprot

JAM-A as a potential surface marker of human pluripotent stem cells

Sarah A. Konze [a,*], Julia Beimdiek [b], Astrid Oberbeck [c], Falk F.R. Buettner [b,c,**]

[a] Institute for Molecular and Cell Physiology, Hannover Medical School, 30625 Hannover, Germany
[b] Proteomics, Institute of Theoretical Medicine, Faculty of Medicine, University of Augsburg, 86159 Augsburg, Germany
[c] Institute of Clinical Biochemistry, Hannover Medical School, 30625 Hannover, Germany

ARTICLE INFO

Keywords:
Human pluripotent stem cells
Embryoid body-based differentiation
Proteomics
Cell surface marker
JAM-A

ABSTRACT

Human pluripotent stem cells can be differentiated into a variety of different cell types, for instance cardiomyocytes. Especially in the context of future application in regenerative medicine, it is crucial to understand the developmental processes taking place upon differentiation. Moreover, the identification of a panel of cell surface markers suitable for characterization and purification is necessary to ensure quality of human pluripotent stem-cell derived products. In this study, we used quantitative mass spectrometry to characterize proteomic changes in early mesendodermal differentiation. Two human pluripotent stem cell lines, one embryonic (H3) and one induced pluripotent stem cell line (I2), were analyzed under pluripotent conditions and after two days of embryoid body-based differentiation. Functional clustering and enrichment analysis showed down-regulation of proteins associated with pluripotency and the tricarboxylic acid cycle at day two. In contrast, proteins related to the proteasome and annexin family were up-regulated upon differentiation. Among the proteins that were down-regulated upon differentiation in both, H3 and I2, the membrane protein junctional adhesion molecule A (JAM-A) emerged as potentially associated with pluripotency. Flow cytometry and immunocytochemistry further confirmed down-regulation of JAM-A on the cell surface of human induced pluripotent stem cells that were differentiated toward mesendoderm for just two days.

Statement of significance: Understanding early molecular changes during human pluripotent stem cell differentiation is essential for stem cell biology and regenerative medicine. This study provides a comparative proteomic analysis of two cell lines during early differentiation and identifies coordinated metabolic and pluripotency-associated changes. The understanding of changes that occur in the early phase of cardiomyocyte differentiation might be helpful to more precisely monitor the differentiation process.

Importantly, we identify the membrane protein JAM-A as a robustly down-regulated cell surface protein, highlighting its potential as marker for human pluripotent stem cells. In the future, JAM-A might be used in a panel of cell surface markers for pluripotent stem cells in order to remove pluripotent stem cells from stem cell-derived therapeutic products.

1. Introduction

Human pluripotent stem cells (hPSCs), comprising human embryonic stem cells (hESCs) and human induced pluripotent stem cells (hiPSCs) are promising sources for regenerative applications and individualized medicine [1]. Due to their ability to differentiate into nearly every somatic cell type, hPSCs are of high interest for tissue replacement approaches, particularly for organs with limited inherent regenerative capacity, such as the heart [2]. Over the past decades, considerable efforts have been devoted to refining cardiomyocyte differentiation protocols to direct the in vitro differentiation process toward the efficient generation of purified populations of defined cardiomyocyte subtypes, resulting in substantial recent progress in improving both the yield and subtype specification of cardiomyocytes derived from hPSCs [3]. Cardiomyogenic specification of hPSCs can be achieved through various strategies, including biphasic small molecule–mediated modulation of Wnt signaling [4,5], cytokine-based modulation of key signaling pathways [6] or the use of the p38 MAPK inhibitor SB203580 in combination with insulin depletion [7,8].

We previously investigated proteomic and glycomic changes during

* Corresponding author.
** Corresponding author at: Proteomics, Institute of Theoretical Medicine, Faculty of Medicine, University of Augsburg, 86159 Augsburg, Germany.
E-mail addresses: konze.sarah@mh-hannover.de (S.A. Konze), falk.buettner@med.uni-augsburg.de (F.F.R. Buettner).

https://doi.org/10.1016/j.jprot.2026.105680
Received 21 January 2026; Received in revised form 4 May 2026; Accepted 18 May 2026
Available online 19 May 2026

cardiac differentiation to elucidate the molecular pathways that govern this process and to identify surface markers for hPSC-derived cardiomyocytes [9–13]. Considering the envisioned clinical application of hPSC-derived cardiomyocytes, it is necessary to remove remaining pluripotent stem cells from the generated cell therapy product to exclude severe complications, i.e. formation of teratoma. The list of established hPSC surface markers is still rather short and among them are the cell surface glycans SSEA-3 and SSEA-4 [14], SSEA-5 [15], TRA-1-60 and TRA-1-81 [16]. We recently identified the glycosphingolipid lacto-N-tetraosylceramide (Lc4-Cer) as a hPSC-specific surface molecule and showed that hPSCs can be depleted from differentiated populations by immunological targeting the terminal glycan epitope type 1 LacNAc of Lc4-Cer [17]. Only few cell surface proteins have been described as hPSC-specific, comprising podocalyxin-like protein (PODXL) [18], Claudin-6 [19], Thy-1 (CD90) [20], alkaline phosphatase (ALPL) [21], and EpCAM (CD326) [22]. However, none of these cell surface biomolecules is exclusively restricted to the pluripotent state [23]. Therefore, there is a clear need to further expand the repertoire of molecules characteristic of hPSCs, with the aim of ultimately employing combinatorial marker panels that enable more accurate characterization and more effective targeting of hPSCs within heterogeneous populations of differentiated cells. In this study, we performed a SILAC-based global proteomic comparison [24] between undifferentiated hPSCs and cells at an early stage of cardiac differentiation, using mass spectrometry (MS). This analysis not only expanded the repertoire of known hPSC surface markers but also identified candidate proteins associated with early mesendodermal commitment, which may improve our understanding of this developmental stage and provide tools for process control during differentiation. Among the identified proteins, junctional adhesion molecule A (JAM-A; also known as JAM-1, CD321, or F11R) was markedly down-regulated shortly after the onset of differentiation. This observation was validated using complementary approaches, including quantitative gene expression analysis and flow cytometry. Our findings suggest that JAM-A may serve as a useful marker for distinguishing undifferentiated hPSCs from their mesendodermal derivatives.

2. Experimental procedures

2.1. Cultivation of hPSCs

Two hPSC lines were used in this study: human embryonic stem cells ES03 (ES Cell International, National Cell Bank, Wisconsin, WI, USA), in the following referred to as H3 and in-house generated human induced pluripotent stem cells derived from umbilical cord blood endothelial cells (hCBiPSCs clone 2 [25]), in the following termed I2. Cultivation of pluripotent H3 and I2 was carried out essentially as described previously [26]. Briefly, hPSCs were maintained at 37 °C with 85% relative humidity and 5% CO_2. All culture vessels were purchased from Greiner (Greiner Bio-One, Frickenhausen, Germany) and all tissue culture reagents were purchased from Gibco / Thermo Fisher Scientific (Waltham, MA, USA), if not stated otherwise. hPSCs were cultivated in 6-well-plates on feeder cells, i.e. γ-irradiated human foreskin fibroblasts (CCD919, ATCC, Manassas, VA, USA), in stem cell medium (KnockOut™ DMEM, 20% [v/v] KnockOut™ Serum Replacement, 1% [v/v] MEM Non-Essential Amino Acids (NEAA), 0.5% [v/v] GlutaMAX™, 0.1 mM 2-Mercaptoethanol (2-ME)) supplemented with 10 ng/ml (I2) or 50 ng/ml (H3) basic fibroblast growth factor (bFGF, Institute of Technical Chemistry, Leibniz University Hannover, Hannover, Germany). Passaging was carried out by collagenase IV treatment.

2.2. EB-based differentiation

hPSCs were differentiated for two days in a chemically defined, EB-based approach as described previously [8,11]. To induce EB formation, hPSC colonies from feeder-based culture were detached using a plastic cell scraper and transferred into 6-well suspension culture plates in serum-free (SF) differentiation medium (high glucose DMEM, 1% [v/v] NEAA, 1% [v/v] GlutaMAX™, 0.1 mM 2-ME, 1% [v/v] Insulin-Transferrin-Selenium (ITS) supplement). Cells were allowed to aggregate for 24 h. Subsequently, insulin was removed from the medium by allowing the EBs to settle down, washing once with basic serum-free (bSF) medium, which is SF medium without insulin, and transferring the EBs back to 6-well suspension culture plates in bSF medium supplemented with 10 μM of the p38 mitogen-activated protein kinase inhibitor SB203580 (Jena Bioscience, Jena, Germany). EBs were cultivated for one more day and harvested by centrifugation.

2.3. Monolayer-based mesendodermal differentiation

Mesendodermal differentiation of I2 in a monolayer was performed essentially as described previously by Lian et al. 2012 [4] with minor modifications as stated. Briefly, the cells were cultured for at least three passages under feeder-free conditions on Matrigel® in mTeSR1™ (STEMCELL™ Technologies, Vancouver, Canada) medium before the beginning of the differentiation, which was initiated from cells seeded on a 6-well plate coated with Matrigel® in mTeSR1™ medium (d-3). Cells were refreshed with mTeSR1™ on day −2 and day-1. Differentiation was initiated on d0 by replacing medium to RPMI (RPMI 1640) including GlutaMAX™, 2% (v/v) B27™ minus insulin and 9 μM CHIR99021 (Selleckchem, Houston, TX). After 24 h (d1) the medium was replaced by RPMI/B27™ minus insulin without supplements. 48 h later (d3) the medium was refreshed with RPMI/B27™ minus insulin supplemented with 5 μM IWP-4 (STEMCELL™ Technologies). On d5, the medium was again replaced by RPMI/B27™ minus insulin without supplements. Cell harvest for flow cytometry was performed on d0, d2 and d7.

2.4. SILAC labeling of hPSCs

For SILAC labeling, the DMEM component of the stem cell medium and the differentiation medium was replaced by DMEM-F12 for SILAC and DMEM for SILAC (both from Thermo Fisher Scientific, Waltham, MA, USA), respectively. DMEM F-12 for SILAC was supplemented with 7×10^{-4} mol/l of the respective arginine (Arg) isotopologue (Arg-6 = L-[$^{13}C_6$] Arg-HCl, referred to as "medium" Arg or Arg-10 = L-[$^{13}C_6^{15}N_4$] Arg-HCl, referred to as "heavy" Arg) and 5×10^{-4} mol/l of the respective lysine (Lys) isotopologue (Lys-4 = L-[$^{2}H_4$] Lys-HCl, referred to as "medium" Lys or Lys-8 = L-[$^{13}C_6^{15}N_2$] Lys-HCl, referred to as "heavy" Lys) (Silantes, Munich, Germany). DMEM for SILAC was supplemented with 4×10^{-4} mol/l Arg-6 and 8×10^{-4} mol/l Lys-4 as "medium" or 4×10^{-4} mol/l Arg-10 and 8×10^{-4} mol/l Lys-8 as "heavy" condition.

2.5. Sample preparation for mass spectrometry

For each MS sample, two to three wells of a six well plate of hPSCs or EBs were washed twice with 1× PBS (AppliChem, Darmstadt, Germany), detached by scraping, if adherent, and pooled. Cells were pelleted by centrifugation and washed again with 1× PBS. Cell lysis was performed in ice-cold RIPA-buffer (50 mM Tris-HCl, pH = 8.0 with 1.0% [v/v] NP-40 [Roche, Basel, Switzerland], 0.5% [w/v] sodium deoxycholate [Sigma Aldrich, St. Louis, MO, USA], 0.1% [w/v] sodium dodecylsulfate [SDS, Sigma Aldrich] and 150 mM NaCl with 1 mM PMSF (Roche, Mannheim, Germany) and 1% HALT protease inhibitor cocktail (Thermo Fisher Scientific)) by sonification in a cup horn for two cycles of 1 min and 30 s, respectively, using a Branson Sonifier 450 with settings for output control at 5 and duty cycle at 50%. Subsequently, cell debris was removed by centrifugation at 10,000 x*g* for 2 min. The protein concentration was determined using the Pierce 660 nm protein assay reagent (Thermo Fisher Scientific). Volumes containing corresponding protein amounts of two differently labeled SILAC samples were pooled and precipitated in the four-fold volume of acetone at

−20 °C o/n. The pelleted protein was resuspended in Laemmli buffer (35 mM Tris-HCl pH 6.8, 7% [v/v] glycerol, 2.8% [w/v] SDS and 0.005% [w/v] bromophenol blue) and separated on a 10% SDS polyacrylamide gel. Gels were stained using Roti-Blue® Coomassie dye (Roth, Karlsruhe, Germany) and the sample lanes were manually sliced into small pieces of about 1 mm^3 that were subjected to tryptic in-gel digestion and subsequent peptide extraction as described previously (Konze et al., 2014) according to the method presented by Shevchenko et al., 2006 [27]. Extracts were dried by vacuum centrifugation and dissolved in an aqueous solution of 2% ACN and 0.1% trifluoroacetic acid (TFA, Sigma Aldrich). After agitation for 20 min (900 rpm, Eppendorf thermomixer) and subsequent centrifugation at 13.000 x*g* for 5 min the supernatants were subjected to mass spectrometry.

2.6. LC-MS/MS analysis

LC-MS/MS analysis of extracted peptides was performed essentially as described previously [11,28]. A nano-flow ultra-high pressure liquid chromatography system with reversed phase chromatography (RSLC, Thermo Fisher Scientific) was coupled online via a Nano Spray Flex Ion Source II (Thermo Fisher Scientific) to an LTQ-Orbitrap Velos mass spectrometer (Thermo Fisher Scientific). Acquisition of overview scans was performed at a resolution of 60 k at *m/z* 400 in a mass range of *m/z* 300–1600 in the orbitrap analyzer and stored in profile mode. Of the ions with double or triple charge and a minimum intensity of 2000, the ten with the highest intensity were selected for CID fragmentation with a normalized collision energy of 38.0, an activation time of 10 ms and an activation Q of 0.250 in the LTQ. Fragment ion mass spectra were recorded in the LTQ at normal scan rate and stored as centroid *m/z* value and intensity pairs. Active exclusion was set so that ions fragmented once were excluded from further fragmentation for 70 s within a mass window of 10 ppm of the specific *m/z* value.

2.7. Processing of MS data

Processing of raw data was performed as described previously [11] using the MaxQuant proteomics software suite [29] version 1.2.0.16 for identification and quantification of proteins. The implemented Andromeda [30] search engine v1.1.0.36 was used to search generated peak lists against the human entries of the IPI protein data base (ipi.HUMAN.v3.68; 87,083 entries) setting the false discovery rate to 1% for proteins and peptides. The following modifications were set: oxidation on methionine and *N*-acetylation as variable modification and carbamidomethylation as fixed modification. Peptides with and without modifications were allowed for quantification. A maximum of two missed cleavages of trypsin (cleavage C-terminal of K, R) were allowed. Mass tolerance for precursor ions and fragment ions was set to 20 ppm and 0.5 Da, respectively. Known contaminants were excluded from the protein lists. Proteins were only stated to be identified, if at least two peptides and among them one unique or razor peptide per protein with a minimum peptide length of six amino acids were found. A false discovery rate of 0.01 on protein and peptide level and the re-quantification mode was allowed. Protein ratios were calculated from razor and unique peptides only for hPSCs vs. d2 differentiations and log2-transformed. An unpaired, two-sided, heteroscedastic Student's *t*-test was applied and an unadjusted *p*-value <0.05 was set as threshold for significant changes of protein intensities. All proteins identified and quantified in this study are listed in Supplemental Table 1.

2.8. Biostatistical analysis of MS data

The freely accessible software package MeV (MultiExperiment Viewer) version 4.8.1 [31], retrieved from http://www.tm4.org/mev.html, was used to perform hierarchical clustering of proteins applying the following settings: linkage method: average linkage analysis; leaf order optimization: genes; distance metric selection: Pearson uncentered. Gene ontology analysis for KEGG pathways was conducted applying the *Search Tool for the Retrieval of Interacting Genes/Proteins* (STRING, www.string-db.org, accessed: January 12, 2024) searching for *homo sapiens* proteins.

2.9. Isolation of total RNA and cDNA synthesis

Undifferentiated hPSCs or EBs from one or two wells of a 6-well plate were collected in adequate volumes of TriZOL™ (Life Technologies) and stored at −80 °C until further processing. Extraction of RNA from the aqueous phase harvested after addition of chloroform was performed as described previously [26] with NucleoSpin® RNA II isolation columns (Macherey & Nagel, Düren, Germany) according to the manufacturer's instructions.

2.5 μg total RNA per sample were used to carry out cDNA synthesis as described [26] and synthesized cDNA was used in a 1:10 dilution for qPCR.

2.10. Quantitative real-time PCR

Quantitative real-time PCR (qPCR) was performed as described previously [26] on a 7500 Fast Real-time PCR System (Applied Biosystems) using sealed 96-well optical reaction plates (Applied Biosystems). SYBR Green Nucleic Acid Stain (Life Technologies) was used as reporter system. Relative expression of target genes was determined by normalization to beta-actin (*ACTB*). A cDNA mix composed of cDNA from hPSCs grown under feeder-free conditions as described in [26] was used as reference sample throughout all PCR runs of the respective target genes to account for inter-run variations. For stem cell marker expression, this reference mix was a pool of feeder-free cultivated I2 and H3. C_T values were determined automatically by the 7500 Software v2.0.5. Relative expression was calculated using the $\Delta\Delta C_T$ method, where the relative expression is $= 2^{-\Delta\Delta C}_T$ and the reference sample was set =1. Sequences of oligonucleotides used as primers in qPCR analyses are listed in Supplemental Table T2.

2.11. Immunofluorescence microscopy

For immunofluorescence microscopy (IF) of hPSCs, the cells were passaged into 3.5 cm dishes on a feeder cell layer or on Matrigel™ as described above and grown until they reached the desired colony size.

Fixation was carried out by incubation with 4% paraformaldehyde (AppliChem) in PBS for 30 min. Fixed cells were blocked with 2% BSA / PBS for 20 min. Only if intracellular epitopes were to be stained, 0.1% [v/v] Triton X-100 (ICN Biomedicals, Aurora, OH, USA) was added to the blocking reagent. Primary and secondary antibodies were diluted in 2% BSA / PBS with or without 0.1% [v/v] Triton X-100 and incubated at room temperature for 1 h each. Primary and secondary antibodies used for immunofluorescence analysis and the respective dilutions are listed in Supplemental Table T3. Nuclei were counterstained with Hoechst 33258 (AppliChem) 1:4000 diluted with PBS. After staining, plastic dishes were covered with cover slips applying one droplet of Fluorescence Mounting Medium (Dako Deutschland GmbH, Hamburg, Germany). Microscopy was performed using a Zeiss Axiovert 200 M microscope with Axio MRm camera and Axio Vision software v4.7 (Zeiss, Oberkochen, Germany).

2.12. Flow cytometry

For flow cytometry (FC), cells were washed twice with PBS and treated with Accutase (Thermo Fisher Scientific) for 5 min at 37 °C. Singularized cells were fixed with 4% PFA, washed with once PBS and stained with antibodies in FACS buffer (1% BSA in PBS) for 45 min on ice. 50000 cells were stained per sample. Negative and isotype controls were made from a pool of cells of all time points. Washing after antibody staining was performed twice with the five-fold volume of FACS buffer.

Subsequently, cells were resuspended in 0.5 mL FACS buffer, filtered through a 70 µm mesh, diluted with 1 mL PBS and analyzed applying a CyFlow ML flow cytometer (Partec GmbH, Münster, Germany) and Flowing Software 2 (Perttu Terho, Turku Centre for Biotechnology, Turku, Finland). Antibodies for flow cytometry are listed in Supplemental Table T3.

3. Results

3.1. SILAC-labeled hPSCs retain pluripotency and remain responsive to differentiation cues

In this study, we employed a SILAC-based quantitative proteomics approach to compare hPSCs with their derivatives collected at day 2 of mesendodermal differentiation (d2). We used two hPSC lines throughout this study: one human embryonic stem cell (hESC) line (H3) and one human induced pluripotent stem cell (hiPSC) line (I2). To ensure efficient incorporation of medium- or heavy-labeled amino acids for SILAC, cells were cultured in SILAC medium for at least three passages prior to the start of the experiment and maintained in the same medium throughout the two-day differentiation period as (schematically shown in Fig. 1). For the hPSC lines used in this study, we previously showed that SILAC-labeling did not negatively interfere with the levels of pluripotency-related markers [26]. Furthermore, it was also confirmed before that the hPSC samples exhibited sufficient SILAC-labeling efficiency for reliable quantitative analysis [26]. qPCR analysis was performed on the d0 and d2 samples used in the MS experiments to quantify transcript levels of key pluripotency markers, including *OCT3/4, NANOG*, *LIN28*, and *SOX2* (Fig. 2A). Moreover, we analyzed lineage markers for the three germ layers, i.e. endoderm (*FOXA2* [32] and *SOX17* [33]), ectoderm (*PAX6* [34] and *NES* [35]) and mesoderm (*T/BRA* [36] and *MESP1* [37]) (Fig. 2B). All pluripotency markers tested showed a slight down-regulation in d2-EBs compared to d0-hPSCs (Fig. 2A). As expected, mesodermal and endodermal markers were strongly up-regulated on d2 vs. d0, suggesting initiation of differentiation toward a mesendodermal lineage. Concomitantly, expression levels of neuroectodermal markers increased slightly (Fig. 2B).

3.2. Proteomic and biostatistical analysis of d2 versus d0

To quantitatively determine changes in the proteome caused by early induction of mesendodermal differentiation, hPSCs (d0) were compared with derived EBs (d2) by SILAC-based proteomics. Two hPSC lines (H3, I2) were grown under SILAC-conditions as biological triplicates at each time point, respectively. Samples of different time points (d0 and d2) and with different SILAC-labels (medium and heavy) were pooled as illustrated in the schematic overview of the experimental setup (Fig. 1). Quantitative proteomic analysis of d0-hPSCs and d2-EBs led to the identification of a total of 2063 proteins. Among these, 1517 proteins were identified based on at least two unique or razor peptides and detected in at least two independent replicates. Of these, 1408 proteins were found in both, H3 and I2 cell lines, while 51 and 58 proteins were exclusively detected in H3 or I2, respectively (Fig. 3A and Supplemental Table T1). To assess the concordance of proteomic changes between the two cell lines, we performed hierarchical clustering of mean fold changes (d2 vs. d0) for the 1408 proteins commonly identified in both datasets. This analysis revealed that most proteins exhibited similar regulation patterns across biological replicates and between cell lines (Fig. 3B). Given that changes during the early phase of differentiation were expected to be relatively subtle, a threshold of 1.25-fold regulation was applied for downstream analysis. Using Student's *t*-test ($p < 0.05$), we identified 66 up-regulated and 68 down-regulated proteins in H3 cells that exceeded this fold-change cutoff. In I2 cells, 25 proteins were significantly up-regulated and 54 down-regulated by more than 1.25-fold. To directly compare proteomic changes between the two cell lines, we plotted the $\log_2$-transformed average fold changes of significantly ($p < 0.05$ in at least one cell line) regulated proteins in H3 and I2 cells against each other (Fig. 3C). Of these, 75 proteins were consistently up-regulated and 57 consistently down-regulated in both, H3 and I2 cells. Notably, only two proteins, – UBC (ubiquitin C) and D6S218E (40S ribosomal protein S18) - were significantly up-regulated on day 2 in both cell lines (H3 and I2). On the other hand, 14 proteins were significantly down-regulated in both H3 and I2 cells. Among these, four proteins - PEPCK2, ALDH1B1, PDHB, and ACO2 - are involved in glucose metabolism pathways. Additionally, the cell surface protein JAM-A (also

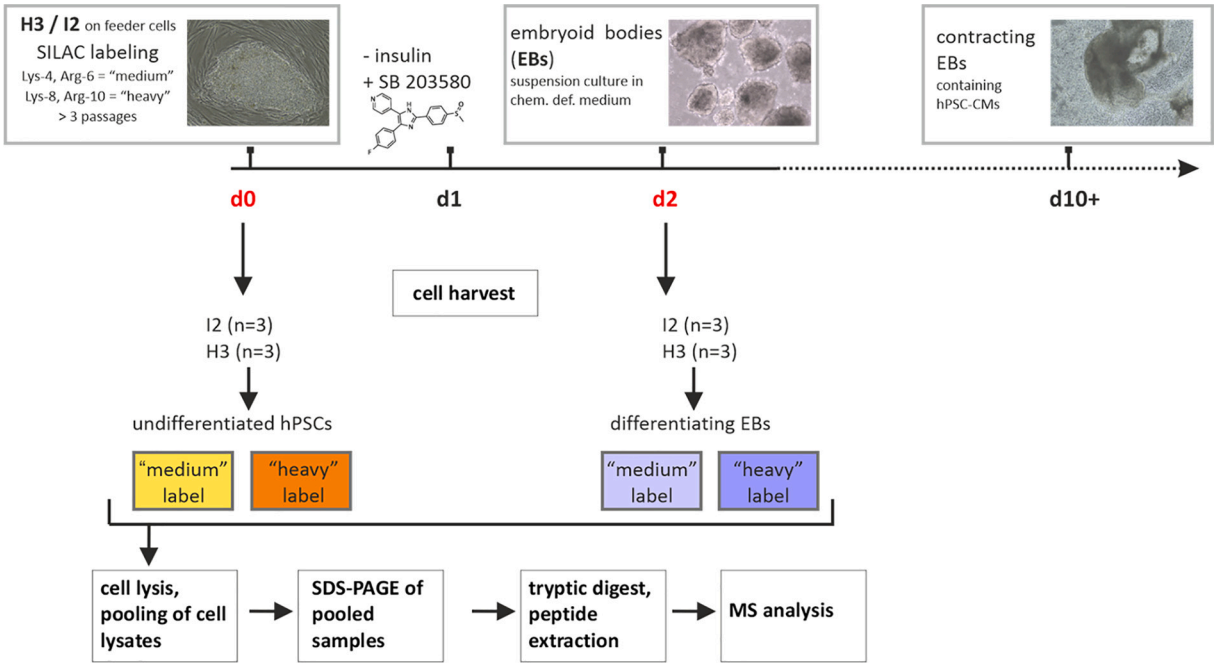

Fig. 1. Experimental workflow. Pluripotent H3 and I2 cells were cultured on feeder layers, SILAC-labeled, and differentiated under SILAC conditions as embryoid bodies for two days in a chemically defined, serum-free medium. For each cell line and time point, three biological replicates were harvested as indicated, pooled, and subjected to mass spectrometry analysis.

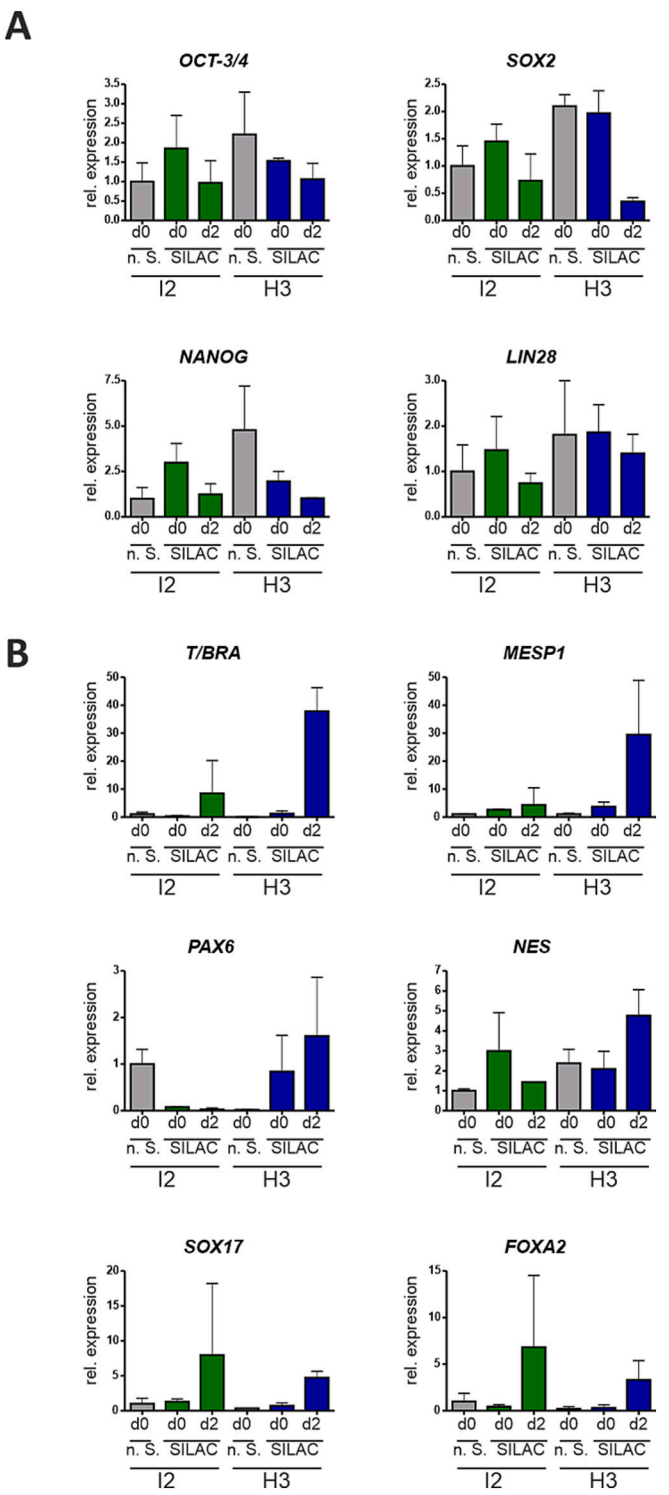

Fig. 2. qPCR analysis confirms loss of pluripotency and initiation of mesendodermal differentiation in H3 and I2 cells. SILAC-labeled H3 and I2 cells were analyzed at day 0 (d0) and after 2 days of embryoid body (EB) differentiation (d2). *A*, Relative expression of the pluripotency markers *OCT-3/4*, *SOX2*, *NANOG*, and *LIN28*. B, Relative transcript levels of mesodermal (*T/BRA*, *MESP1*), ectodermal (*PAX6*, *NES*), and endodermal (*FOXA2*, *SOX17*) markers comparing d2 EBs with d0 hPSCs. Non-SILAC-labeled I2 cells were used as the reference sample. Data represent $n = 3$ biological replicates per condition. Values are shown as mean +/− standard deviation.

known as JAM-1, F11R, or CD321) was consistently down-regulated on day 2 in both datasets. Collectively, these findings indicate that the overall pattern of protein regulation is largely conserved between the H3 and I2 cell lines (Fig. 3C).

3.3. Gene ontology analysis using STRING

Proteins that were significantly regulated ($p < 0.05$) by more than 1.25-fold (up- or down-regulated) in either H3 or I2 cells upon comparison of day 2 with day 0 were subjected to cluster as well as gene ontology (GO) enrichment analysis using the open-access STRING database. (Fig. 4). For the down-regulated proteins, STRING analysis revealed a cluster of proteins belonging to the mitochondrial matrix and especially the citrate cycle. This finding is reflected upon GO enrichment analysis for KEGG pathways revealing the second-highest strength for "TCA cycle" (hsa00020, Supplemental Table T4 and Supplemental Fig. S1A). Moreover, pluripotency-associated proteins, i.e. DNMT3A, DNMT3B, DPPA4 and TRIM71 as well as proteins belonging to the ribosome and the splicing machinery formed a cluster in the STRING analysis of down-regulated proteins (Fig. 4A). For the up-regulated proteins, the STRING analysis showed strong clustering for proteasome components which also had the highest strength within this group upon GO enrichment analysis (Supplemental Table T5 and Supplemental Fig. S1B). A further cluster is built by annexins/phospholipase inhibitor and a third by translation-related proteins being enriched (Fig. 4B).

3.4. JAM-A levels are decreased upon early onset of mesendodermal differentiation

In addition to providing a global view of proteomic alterations associated with mesendodermal differentiation of hPSCs, we screened the dataset for potential cell surface biomarkers characteristic of the pluripotent state, defined as surface proteins whose abundance was substantially reduced between day 0 and day 2. To this end, proteins that were significantly down-regulated ($p < 0.05$, fold change >1.25) in either H3 or I2, or in both cell lines were filtered for annotations indicating plasma membrane localization using UniProt (accessed January 24, 2024). This approach yielded 10 candidate proteins, whose fold-change values and peptide counts are summarized in Table 1. Among these, JAM-A emerged as a particularly compelling candidate, as it was significantly down-regulated in both pluripotent stem cell lines (H3 and I2) as early as two days after induction of mesendodermal differentiation. Together with its established cell surface localization [38], this profile suggested JAM-A as a potential marker of the pluripotent state.

To independently assess the observed decrease in JAM-A abundance, we employed a set of orthogonal, non-proteomic approaches, including qPCR, immunofluorescence staining, and flow cytometry. First, *JAM-A* transcript levels were analyzed in I2 cells collected at day 0, day 2, and day 7 of EB-based cardiomyogenic differentiation and compared with those of the established pluripotency marker *OCT-3/4*. *JAM-A* expression was strongly reduced already at day 2, with a more pronounced decrease than observed for OCT-3/4. While *OCT-3/4* expression continued to decline by day 7, *JAM-A* transcript levels remained relatively stable between days 2 and 7 (Fig. 5A).

For immunocytochemical analysis, JAM-A and OCT-3/4 were examined using a monolayer-based differentiation protocol involving temporal modulation of Wnt signaling, as described by Lian et al. [4]. Compared with EB-based differentiation, this two-dimensional culture system facilitates improved antibody accessibility. In pluripotent cells (day 0), immunofluorescence staining demonstrated clear cell surface localization of JAM-A and nuclear localization of OCT-3/4. Upon differentiation (day 2), signal intensities for both markers were markedly reduced (Fig. 5B).

Finally, flow cytometric analysis using JAM-A–specific antibodies was performed on I2 cells at the pluripotent stage (day 0) and after 2 and

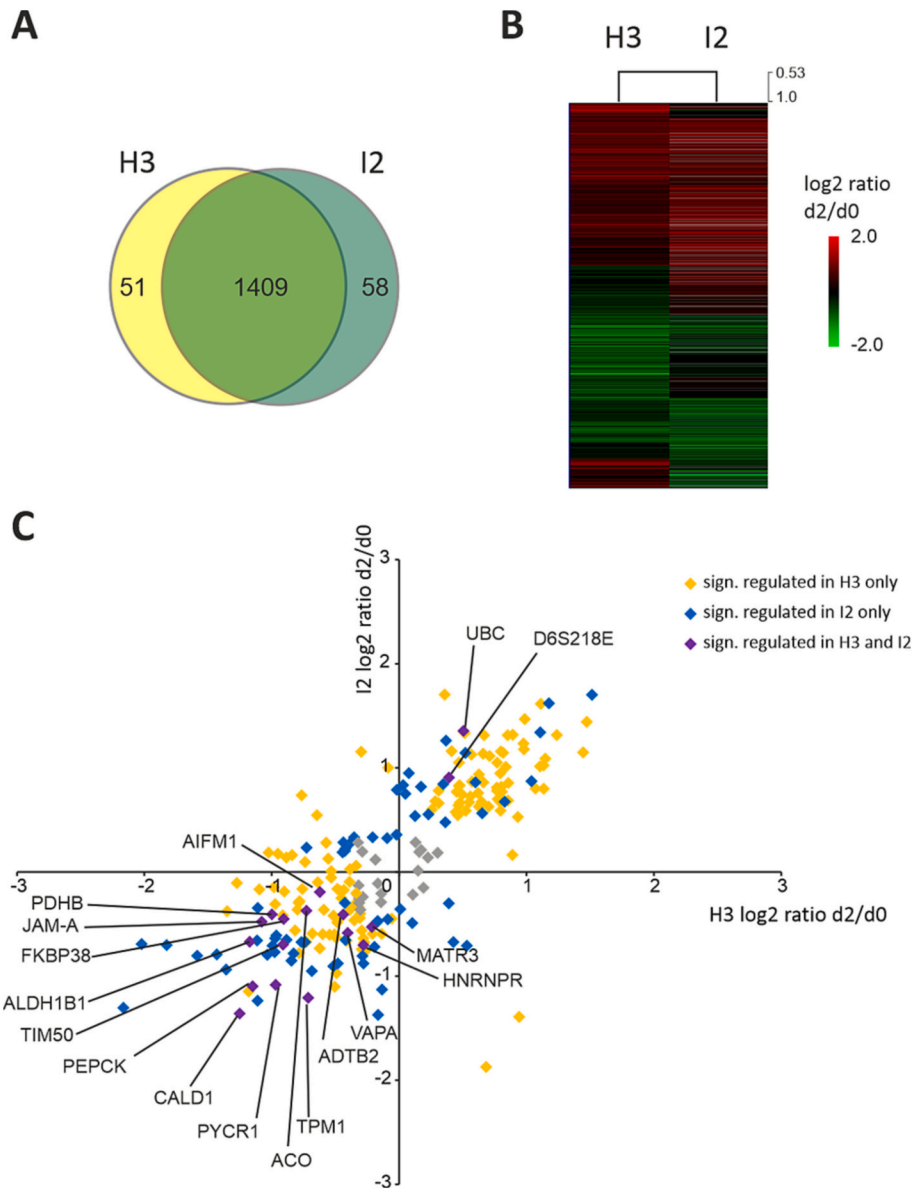

Fig. 3. Comparative proteomic analysis of H3 and I2 cells. *A*, Venn diagram showing the overlap of proteins identified in the pooled samples of H3 and I2 cells. *B*, Heatmap displaying mean protein regulation ratios in H3 and I2 sample pools, generated by hierarchical clustering using the open-access MultiExperiment Viewer. All proteins identified in both, H3 and I2 are presented with mean values of log2-transformed regulation ratios of d2/d0. C, Correlation analysis of significantly regulated proteins in H3 and I2 cells. Only proteins identified in both cell lines (H3 and I2) and significantly regulated ($p < 0.05$) in H3 (yellow), I2 (blue), or in both cell lines (H3 and I2, purple) are shown. Log_2-transformed average regulation ratios for H3 and I2 cells are plotted on the X- and Y-axes, respectively. (For interpretation of the references to colour in this figure legend, the reader is referred to the web version of this article.)

7 days of monolayer-based mesendodermal differentiation. This analysis revealed a pronounced reduction in JAM-A surface abundance at both differentiation time points (Fig. 5C).

Taken together, these independent experimental approaches consistently demonstrate a rapid and sustained loss of JAM-A upon mesendodermal differentiation.

4. Discussion

In this study, we set out to gain deeper insight into biological processes at the early phase of human pluripotent stem cell differentiation. Therefore, we quantitatively interrogated whole cell proteomes of hPSCs and derived cells only two days after mesendodermal induction, representing the initial phase of cardiac differentiation, by SILAC. We acknowledge that the proteomics workflow used does not reflect the most recent technological advances. However, it is robust and provides reliable quantitative data. Despite potentially lower proteome depth compared to newer methods, the dataset shows sufficient coverage and reproducibility to support our conclusions. Key findings were consistent across replicates and confirmed by orthogonal validation. Although hESCs and hiPSCs are generally considered to be rather similar, on the proteomic level small but meaningful differences have been identified in the past [39]. Thus, to ensure broader applicability of our findings, one human embryonic stem cell (hESC) line (H3) and one human induced pluripotent stem cell (hiPSC) line (I2) was used for the proteomics screen in this study.

Our quantitative proteomics approach revealed several pluripotency-associated proteins that were slightly down-regulated on day 2 of differentiation. This observation was corroborated by targeted gene expression profiling of core pluripotency-associated transcription factors (*OCT3/4*, *SOX2*, *NANOG*, *LIN28*) which were also slightly down-regulated after two days of mesendodermal induction. On the other

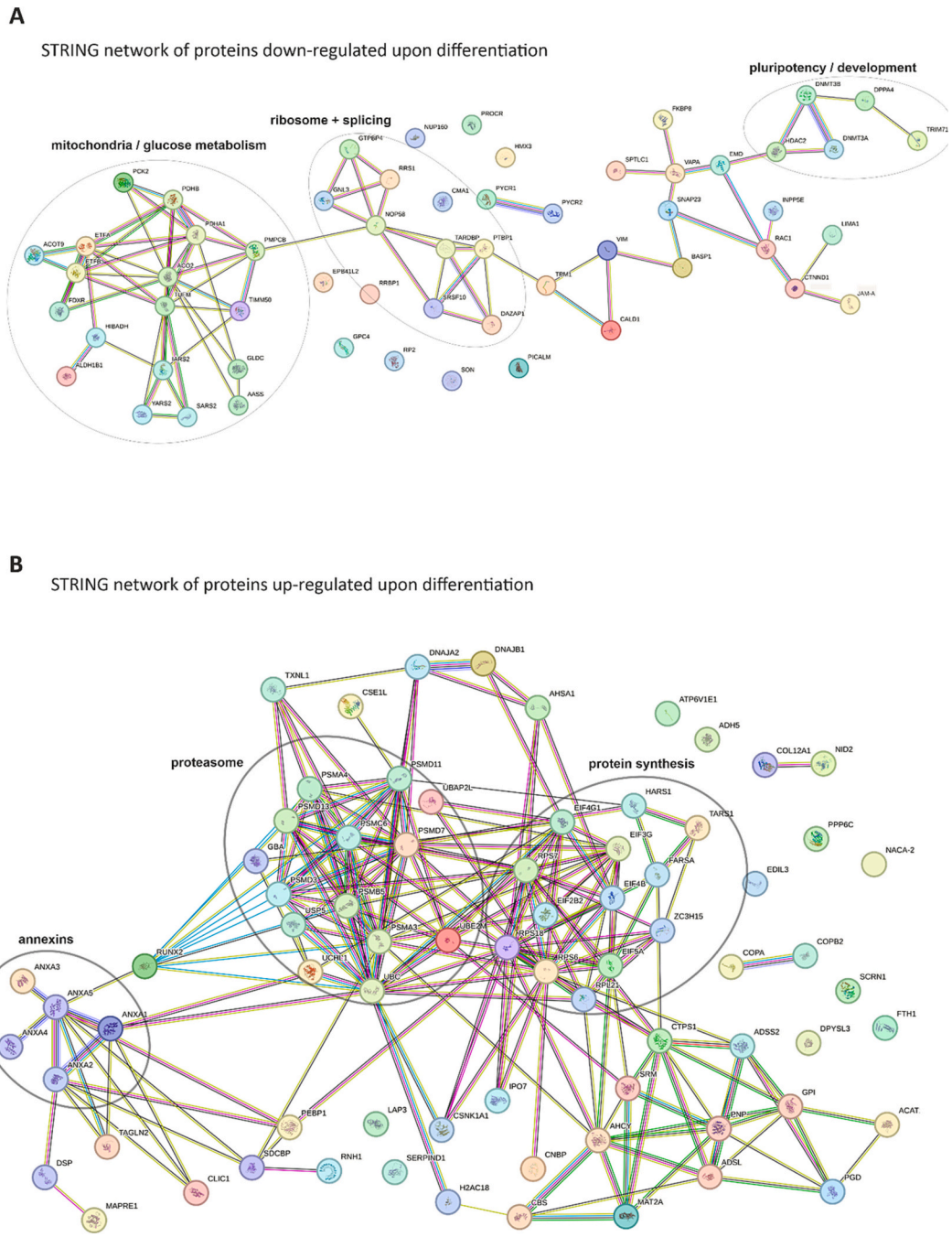

Fig. 4. Protein interaction networks of differentiation-associated proteomic changes. *A*, Network of proteins down-regulated upon differentiation. *B*, Network of proteins up-regulated upon differentiation. Protein-protein interaction networks were generated using the open-access STRING database. All proteins that were significantly down (Fig. 4A) or up-regulated (Fig. 4B) more than 1.25-fold in either H3 or I2 or in both (H3 and I2) were subjected to STRING network clustering for KEGG pathways.

hand, endodermal (*FOXA2*, *SOX17*) and mesodermal (*T*, *MESP1*) markers were strongly increased comparing d2 vs. d0. These findings are in accordance with previous reports highlighting that after induction of differentiation pluripotency markers are for quite some time co-expressed with differentiation markers whose expression strongly increased [40]. A recent study showed that the gene expression levels of the mesendodermal marker *T/Brachyury* already increased at about 12 h upon induction while expression of the pluripotency markers *NANOG* and *SOX2* remained rather constant for up to 24 h and for *OCT-3/4* even for up to 36 h of differentiation [41].

Already two days after induction of differentiation, we observed changes in the proteome reflecting the cellular adaptation during differentiation. Proteins of the TCA cycle and pyruvate metabolism (PDHA1, PDHB, ACO2, ALDH1B1) but also mitochondrial proteins (e.g. PMPCB, TIMM50, TUFM, ETFA, ETFB) with functions distinct from the TCA cycle were reduced on d2. The energy metabolism of hPSCs is well known to depend on a high rate of glycolysis (Warburg effect) rather than oxidative phosphorylation and accordingly hPSCs have few and immature mitochondria [42]. Using quantitative proteomics (iTRAQ with μLC-MS/MS), a decrease of proteins belonging to glycolysis has been observed during the first 48 h of differentiation [43]. Although differentiation is generally associated with an increase in mitochondrial number and function [43], a transitional phase has been postulated, in which the mitochondrial biomass temporarily decreases before

Table 1
Cell surface-located proteins down-regulated upon differentiation.

Protein name	UniProt ID	Gene name	Mean ratio d2/d0	t-Test *p*-value	Identified in x of 6 replicates	# of identified peptides	GO annotation cellular compartment
CD109 antigen, C3 and PZP-like alpha-2-macroglobulin domain-containing protein 7	Q6YHK3	CD109, CPAMD7	**0,37**	**0,048**	3	2	cell surface, extracellular space, plasma membrane
Brain acid soluble protein 1, Neuronal axonal membrane protein NAP-22	P80723	BASP1, NAP22	**0,45**	**0,001**	4	8	plasma membrane, nucleus, cytoskeleton
CD9 antigen, Tetraspanin-29	P21926	CD9, TSPAN29	**0,64**	**0,043**	5	3	extracellular space, plasma membrane, vesicle
Mitochondrial-processing peptidase subunit alpha	Q10713	INPP5E, PMPCA	**0,55**	**0,005**	5	6	extracellular space, mitochondrion
Band 4.1-like protein 2	O43491	EPB41L2	**0,66**	**0,001**	6	5	plasma membrane, nucleus cytoskeleton
Methylsterol monooxygenase 1	Q15800	DESP4, MSMO1	**0,40**	**0,027**	3	2	plasma membrane, endoplasmic reticulum
Desmoglein-2	Q14126	CDHF5, DSG2	**0,64**	**0,018**	5	7	cell surface, plasma membrane, vesicle
Catenin delta-1	O60716	CTNND1	**0,62**	**0,003**	6	18	plasma membrane, cell projection, nucleus, vesicle, synapse
Monocarboxylate transporter 1	P53985	SLC16A1	**0,62**	**0,000**	5	6	plasma membrane, mitochondrion, centrosome
Junctional adhesion molecule A	Q9Y624	F11R, JAM1	**0,58**	**0,003**	6	6	plasma membrane, cytoskeleton, vesicle
Guanine nucleotide-binding protein-like 3, Nucleostemin	Q9BVP2	GNL3	**0,61**	**0,002**	6	5	extracellular space, nucleus, nucleolus
E-cadherin	Q9UII7	CDH1	**0,61**	**0,005**	6	6	cell surface, extracellular region, plasma membrane, endosome, vesicle
Epithelial protein lost in neoplasm beta variant	Q53GG0	EPLIN	**0,49**	**0,006**	4	5	plasma membrane, cytoskeleton
Podocalyxin, GCTM-2 antigen	O00592	PCLP	**0,56**	**0,026**	6	10	extracellular space, plasma membrane, cell projection, filopodium, vesicle
Glypican-4	O75487	GPC4	**0,53**	**0,004**	6	14	extracellular space, extracellular matrix, plasma membrane, nucleus
Guanine nucleotide-binding protein G (q) subunit alpha	P50148	GAQ	**0,65**	**0,024**	2	5	plasma membrane, vesicle
Intercellular adhesion molecule 1	P05362	ICAM1	**0,54**	**0,044**	4	5	cell surface, extracellular space, plasma membrane, vesicle
Protein arginine methyltransferase NDUFAF7, mitochondrial, midA homolog	Q7L592	C2orf56, NDUFAF7	**0,41**	**0,009**	3	5	extracellular space, mitochondrion
Protein XRP2	O75695	RP2	**0,57**	**0,001**	3	2	plasma membrane, cell projection, Golgi apparatus
Caldesmon	Q05682	DKFZp779D0769, CALD1	**0,40**	**0,000**	6	28	plasma membrane, organelle, cytoskeleton
Telomere-associated protein RIF1	Q5UIP0	RIF1	**0,34**	**0,023**	4	5	plasma membrane, nucleus
Vesicle transport-related protein isoform a variant	A8MVJ7	SCFD1	**0,64**	**0,012**	4	6	plasma membrane, vesicle
Ras-related protein R-Ras2	P62070	RRAS2	**0,64**	**0,011**	6	5	plasma membrane, endoplasmic reticulum, vesicle
Synaptosomal-associated protein 23	O00161	SNAP23	**0,58**	**0,001**	5	2	plasma membrane, cell projection, lysosome, vesicle
Vimentin	P08670	VIM	**0,62**	**0,029**	6	63	plasma membrane, cell projection, peroxysome, vesicle

mitochondria are getting fully activated [44]. The reduction of mitochondrial proteins observed in our dataset might be linked to this temporal reduction of mitochondrial mass. Such a transitional phase which likely deserves degradation of the pluripotency-characteristic protein architecture and adaptation to the new cell fate by synthesis of a different specific protein repertoire can be well correlated to the observed increase of proteasomal proteins and also of proteins belonging to the transcription, splicing and translation machinery. In addition, the shift from 2D-monolayer culture to 3D-culture in spheroids requires vast restructuring. These findings are in congruence with our previous data [26], where the proteasome components were also significantly enriched in KEGG pathway analysis upon 20 days of cardiac differentiation.

We further identified 10 different cell membrane proteins that were consistently down-regulated in I2 and H3. Cell surface proteins whose levels decline as early as two days after differentiation induction – at a stage when core pluripotency markers are often still detectable [41] - are of particular interest as candidate markers of the pluripotent state. Such markers are highly relevant, as they not only enable the monitoring of cellular identity but also provide a means to eliminate residual undifferentiated hPSCs from differentiated cell preparations prior to clinical application. Residual hPSCs pose a significant risk due to their potential to form teratomas [45]. The cell surface proteins podocalyxin-like protein (PODXL) [18], Claudin-6 [19], Thy-1 (CD90) [20], alkaline phosphatase (ALPL) [21], and EpCAM (CD326) [22,46] are often claimed as hPSC-specific. However, none of these proteins are exclusively expressed in pluripotent cells [23]. Accordingly, it is essential to broaden the spectrum of molecules associated with hPSCs, as reliable

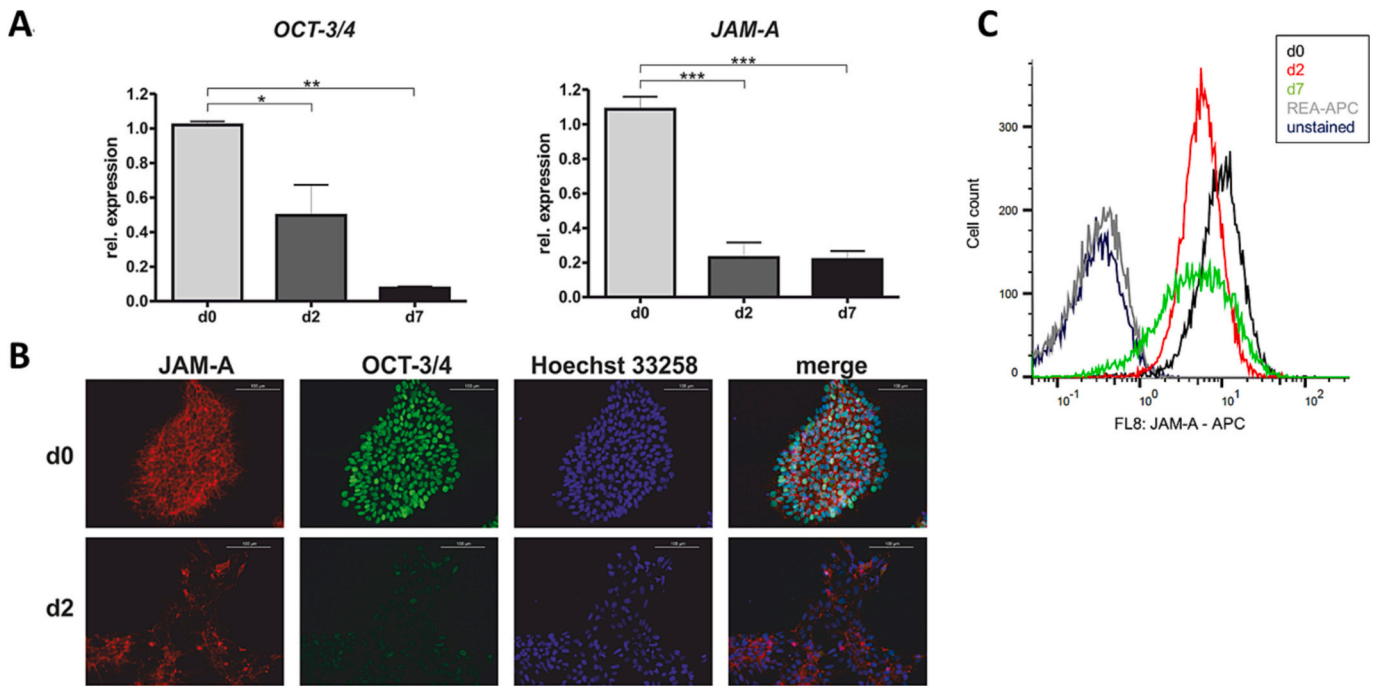

Fig. 5. Rapid down-regulation of JAM-A during mesendodermal differentiation.
A, qPCR analysis of *OCT-3/4* and *JAM-A* expression in hiPSCs at day 0 (d0), day 2 (d2), and day 7 (d7) of EB-based mesendodermal differentiation. One d0 sample was used as the reference. Data represent n = 3 biological replicates per time point. Statistical significance was assessed by one-way ANOVA followed by Bonferroni's multiple-comparison test (*p < 0.05, **$p < 0.01$, ***$p < 0.001$).
B, Immunofluorescence microscopy of hiPSCs at d0 and d2 of monolayer-based mesendodermal differentiation stained for JAM-A (red) and OCT-3/4 (green). Hoechst 33258 was used for nuclear counterstaining. Scale bars, 100 μm.
C-E, Flow cytometry analysis of hiPSCs undergoing monolayer-based mesendodermal differentiation, assessing cell surface levels of JAM-A at d0, d2, and d7. (For interpretation of the references to colour in this figure legend, the reader is referred to the web version of this article.)

identification and selective targeting will ultimately depend on the use of combinatorial marker sets in complex, differentiated cell populations.

Among the identified candidates, JAM-A – a 27 kDa transmembrane glycoprotein (UniProt ID Q9Y624) - was of particular interest. In a previous study comparing undifferentiated I2 and H3 cells with hPSC-derived cardiomyocytes at day 20 of differentiation, we had already observed a greater than fourfold reduction in JAM-A levels upon differentiation [26]. Notably, in this study, down-regulation of JAM-A was observed even shortly after induction of differentiation, which is a prerequisite of a pluripotency marker. Moreover, a non-quantitative cell surface proteomics study identified JAM-A on human and murine ESCs and iPSCs, but not on human foreskin fibroblasts [47]. In line with these observations, Torán et al. reported JAM-A as part of the surface signature of human cardiac progenitor cells, but not of cells in the adult human heart [48]. JAM-A has further been described as a cell surface marker for long-term repopulating hematopoietic stem cells [49] and for proliferative NG2 glia cells in the adult mouse brain [50]. In pathological contexts, elevated JAM-A levels have been associated with poor prognosis in multiple myeloma and glioblastoma patients [51,52]. It has to be considered that the reported presence of JAM-A on other, non-pluripotent cell types, might limit its applicability as pluripotent stem cell marker.

Interestingly, junctional adhesion molecule B (JAM-B), a closely related family member, has previously been described as a potential "stemness" gene [53]. While JAM-A and JAM-B knockout mice are viable and fertile [54,55], deletion of JAM-C - a third JAM family member - results in embryonic lethality in approximately 60% of cases [56], pointing to an important role of JAM proteins in early embryonic development.

Consistent with the proteomics data, gene expression analyses revealed that JAM-A transcript levels were more strongly reduced than those of the canonical pluripotency marker OCT-4 within two days of mesendodermal differentiation. Immunocytochemistry and flow cytometry further demonstrated that JAM-A surface levels are rapidly diminished upon differentiation, underscoring its potential utility as an early indicator of exit from pluripotency. However, it has to be mentioned that this orthogonal validation of JAM-A as a PSC marker was only performed in the hiPSC line I2 and not in the hESC line H3. Since it has been reported that there are meaningful proteomic differences between hESCs and hiPSCs [39], validation of JAM-A in additional cell lines, particularly hESCs would be required before incorporating JAM-A into combinatorial marker panels intended for clinical applications such as residual hPSC depletion.

Taken together, rapid down-regulation of JAM-A upon differentiation suggests that it may complement existing marker panels for comprehensive characterization of hPSCs and may improve strategies aimed at purifying differentiated cell populations for downstream applications.

CRediT authorship contribution statement

Sarah A. Konze: Writing – original draft, Methodology, Investigation, Conceptualization. **Julia Beimdiek:** Visualization, Investigation. **Astrid Oberbeck:** Investigation. **Falk F.R. Buettner:** Writing – original draft, Supervision, Project administration, Funding acquisition, Conceptualization.

Funding

This work was supported by funding from the Deutsche Forschungsgemeinschaft (DFG, German Research Foundation) to F.F.R.B. (BU2920/3–1).

Declaration of competing interest

The authors declare no conflicts of interest.

Acknowlegdements

The authors would like to thank the Core Facility Proteomics at Hannover Medical School headed by Prof. Dr. Andreas Pich for sample analysis and excellent support during data evaluation. We are grateful to Prof. Dr. Scheper (Institute of Technical Chemistry, Leibniz University of Hannover) for providing the ROCK inhibitor Y27632 as well as Prof. Dr. Martin, Dr. Alexandra Haase and Dr. Robert Zweigerdt (LEBAO, MHH) for providing human pluripotent stem cell lines. We also would like to thank Karsten Heidrich and Isabell Niwolik for practical assistance. As part of the manuscript preparation process, the authors employed ChatGPT (OpenAI) as a language-support tool to enhance clarity and readability. The authors reviewed, revised, and approved all content and are solely responsible for the publication.

Appendix A. Supplementary data

Supplementary data to this article can be found online at https://doi.org/10.1016/j.jprot.2026.105680.

Data availability

The mass spectrometry proteomics data have been deposited to the ProteomeXchange Consortium via the PRIDE [1] partner repository with the dataset identifier PXD074454.

References

[1] V. Tabar, L. Studer, Pluripotent stem cells in regenerative medicine: challenges and recent progress, Nat. Rev. Genet. 15 (2) (2014) 82–92.
[2] O. Bergmann, R.D. Bhardwaj, S. Bernard, S. Zdunek, F. Barnabe-Heider, S. Walsh, J. Zupicich, K. Alkass, B.A. Buchholz, H. Druid, S. Jovinge, J. Frisen, Evidence for cardiomyocyte renewal in humans, Science 324 (5923) (2009) 98–102.
[3] D.M. Lyra-Leite, O. Gutierrez-Gutierrez, M. Wang, Y. Zhou, L. Cyganek, P. W. Burridge, A review of protocols for human iPSC culture, cardiac differentiation, subtype-specification, maturation, and direct reprogramming, STAR Protoc 3 (3) (2022) 101560.
[4] X. Lian, C. Hsiao, G. Wilson, K. Zhu, L.B. Hazeltine, S.M. Azarin, K.K. Raval, J. Zhang, T.J. Kamp, S.P. Palecek, Robust cardiomyocyte differentiation from human pluripotent stem cells via temporal modulation of canonical Wnt signaling, Proc. Natl. Acad. Sci. USA 109 (27) (2012) E1848–E1857.
[5] X. Lian, J. Zhang, S.M. Azarin, K. Zhu, L.B. Hazeltine, X. Bao, C. Hsiao, T.J. Kamp, S.P. Palecek, Directed cardiomyocyte differentiation from human pluripotent stem cells by modulating Wnt/beta-catenin signaling under fully defined conditions, Nat. Protoc. 8 (1) (2013) 162–175.
[6] P.W. Burridge, S. Thompson, M.A. Millrod, S. Weinberg, X. Yuan, A. Peters, V. Mahairaki, V.E. Koliatsos, L. Tung, E.T. Zambidis, A universal system for highly efficient cardiac differentiation of human induced pluripotent stem cells that eliminates interline variability, PLoS One 6 (4) (2011) e18293.
[7] X.Q. Xu, S.Y. Soo, W. Sun, R. Zweigerdt, Global expression profile of highly enriched cardiomyocytes derived from human embryonic stem cells, Stem Cells 27 (9) (2009) 2163–2174.
[8] X.Q. Xu, R. Zweigerdt, S.Y. Soo, Z.X. Ngoh, S.C. Tham, S.T. Wang, R. Graichen, B. Davidson, A. Colman, W. Sun, Highly enriched cardiomyocytes from human embryonic stem cells, Cytotherapy 10 (4) (2008) 376–389.
[9] H. Kempf, R. Olmer, A. Haase, A. Franke, E. Bolesani, K. Schwanke, D. Robles-Diaz, M. Coffee, G. Gohring, G. Drager, O. Potz, T. Joos, E. Martinez-Hackert, A. Haverich, F.F.R. Buettner, U. Martin, R. Zweigerdt, Bulk cell density and Wnt/TGFbeta signalling regulate mesendodermal patterning of human pluripotent stem cells, Nat. Commun. 7 (2016) 13602.
[10] S.A. Konze, S. Cajic, A. Oberbeck, R. Hennig, A. Pich, E. Rapp, F.F.R. Buettner, Quantitative assessment of sialo-glycoproteins and N-glycans during cardiomyogenic differentiation of human induced pluripotent stem cells, Chembiochem 18 (13) (2017) 1317–1331.
[11] S.A. Konze, L. van Diepen, A. Schroder, R. Olmer, H. Moller, A. Pich, R. Weissmann, A.W. Kuss, R. Zweigerdt, F.F. Buettner, Cleavage of E-cadherin and beta-catenin by calpain affects Wnt signaling and spheroid formation in suspension cultures of human pluripotent stem cells, Mol. Cell. Proteomics 13 (4) (2014) 990–1007.
[12] C. Rossdam, S.A. Konze, A. Oberbeck, E. Rapp, R. Gerardy-Schahn, M. von Itzstein, F.F.R. Buettner, Approach for profiling of glycosphingolipid glycosylation by multiplexed capillary gel electrophoresis coupled to laser-induced fluorescence detection to identify cell-surface markers of human pluripotent stem cells and derived cardiomyocytes, Anal. Chem. 91 (10) (2019) 6413–6418.
[13] H. Wolling, S.A. Konze, A. Hofer, J. Erdmann, A. Pich, R. Zweigerdt, F.F. R. Buettner, Quantitative Secretomics reveals extrinsic signals involved in human pluripotent stem cell Cardiomyogenesis, Proteomics 18 (14) (2018) e1800102.
[14] B.A. Fenderson, M.P. De Miguel, A.D. Pyle, P.J. Donovan, Staining embryonic stem cells using monoclonal antibodies to stage-specific embryonic antigens, Methods Mol. Biol. 325 (2006) 207–224.
[15] C. Tang, A.S. Lee, J.P. Volkmer, D. Sahoo, D. Nag, A.R. Mosley, M.A. Inlay, R. Ardehali, S.L. Chavez, R.R. Pera, B. Behr, J.C. Wu, I.L. Weissman, M. Drukker, An antibody against SSEA-5 glycan on human pluripotent stem cells enables removal of teratoma-forming cells, Nat. Biotechnol. 29 (9) (2011) 829–834.
[16] P.W. Andrews, G. Banting, I. Damjanov, D. Arnaud, P. Avner, Three monoclonal antibodies defining distinct differentiation antigens associated with different high molecular weight polypeptides on the surface of human embryonal carcinoma cells, Hybridoma 3 (4) (1984) 347–361.
[17] C. Rossdam, S. Brand, J. Beimdiek, A. Oberbeck, M.D. Albers, O. Naujok, F.F. R. Buettner, Targeting the glycan epitope type I N-acetyllactosamine enables immunodepletion of human pluripotent stem cells from early differentiated cells, Glycobiology 34 (4) (2024).
[18] H.L. Tan, W.J. Fong, E.H. Lee, M. Yap, A. Choo, mAb 84, a cytotoxic antibody that kills undifferentiated human embryonic stem cells via oncosis, Stem Cells 27 (8) (2009) 1792–1801.
[19] L. Wang, Y. Xue, Y. Shen, W. Li, Y. Cheng, X. Yan, W. Shi, J. Wang, Z. Gong, G. Yang, C. Guo, Y. Zhou, X. Wang, Q. Zhou, F. Zeng, Claudin 6: a novel surface marker for characterizing mouse pluripotent stem cells, Cell Res. 22 (6) (2012) 1082–1085.
[20] J.S. Draper, C. Pigott, J.A. Thomson, P.W. Andrews, Surface antigens of human embryonic stem cells: changes upon differentiation in culture, J. Anat. 200 (Pt 3) (2002) 249–258.
[21] P.W. Andrews, D.L. Bronson, F. Benham, S. Strickland, B.B. Knowles, A comparative study of eight cell lines derived from human testicular teratocarcinoma, Int. J. Cancer 26 (3) (1980) 269–280.
[22] T.Y. Lu, R.M. Lu, M.Y. Liao, J. Yu, C.H. Chung, C.F. Kao, H.C. Wu, Epithelial cell adhesion molecule regulation is associated with the maintenance of the undifferentiated phenotype of human embryonic stem cells, J. Biol. Chem. 285 (12) (2010) 8719–8732.
[23] P.W. Andrews, P.J. Gokhale, A short history of pluripotent stem cells markers, Stem Cell Rep. 19 (1) (2024) 1–10.
[24] S.E. Ong, B. Blagoev, I. Kratchmarova, D.B. Kristensen, H. Steen, A. Pandey, M. Mann, Stable isotope labeling by amino acids in cell culture, SILAC, as a simple and accurate approach to expression proteomics, Mol. Cell. Proteomics 1 (5) (2002) 376–386.
[25] A. Haase, R. Olmer, K. Schwanke, S. Wunderlich, S. Merkert, C. Hess, R. Zweigerdt, I. Gruh, J. Meyer, S. Wagner, L.S. Maier, D.W. Han, S. Glage, K. Miller, P. Fischer, H.R. Scholer, U. Martin, Generation of induced pluripotent stem cells from human cord blood, Cell Stem Cell 5 (4) (2009) 434–441.
[26] S.A. Konze, S. Werneburg, A. Oberbeck, R. Olmer, H. Kempf, M. Jara-Avaca, A. Pich, R. Zweigerdt, F.F. Buettner, Proteomic analysis of human pluripotent stem cell Cardiomyogenesis revealed altered expression of metabolic enzymes and PDLIM5 isoforms, J. Proteome Res. 16 (3) (2017) 1133–1149.
[27] A. Shevchenko, H. Tomas, J. Havlis, J.V. Olsen, M. Mann, In-gel digestion for mass spectrometric characterization of proteins and proteomes, Nat. Protoc. 1 (6) (2006) 2856–2860.
[28] J. Zeiser, R. Gerhard, I. Just, A. Pich, Substrate specificity of clostridial glucosylating toxins and their function on colonocytes analyzed by proteomics techniques, J. Proteome Res. 12 (4) (2013) 1604–1618.
[29] J. Cox, M. Mann, MaxQuant enables high peptide identification rates, individualized p.p.b.-range mass accuracies and proteome-wide protein quantification, Nat. Biotechnol. 26 (12) (2008) 1367–1372.
[30] J. Cox, N. Neuhauser, A. Michalski, R.A. Scheltema, J.V. Olsen, M. Mann, Andromeda: a peptide search engine integrated into the MaxQuant environment, J. Proteome Res. 10 (4) (2011) 1794–1805.
[31] A.I. Saeed, V. Sharov, J. White, J. Li, W. Liang, N. Bhagabati, J. Braisted, M. Klapa, T. Currier, M. Thiagarajan, A. Sturn, M. Snuffin, A. Rezantsev, D. Popov, A. Ryltsov, E. Kostukovich, I. Borisovsky, Z. Liu, A. Vinsavich, V. Trush, J. Quackenbush, TM4: a free, open-source system for microarray data management and analysis, Biotechniques 34 (2) (2003) 374–378.
[32] M. Levinson-Dushnik, N. Benvenisty, Involvement of hepatocyte nuclear factor 3 in endoderm differentiation of embryonic stem cells, Mol. Cell. Biol. 17 (7) (1997) 3817–3822.
[33] M. Kanai-Azuma, Y. Kanai, J.M. Gad, Y. Tajima, C. Taya, M. Kurohmaru, Y. Sanai, H. Yonekawa, K. Yazaki, P.P. Tam, Y. Hayashi, Depletion of definitive gut endoderm in Sox17-null mutant mice, Development 129 (10) (2002) 2367–2379.
[34] X. Zhang, C.T. Huang, J. Chen, M.T. Pankratz, J. Xi, J. Li, Y. Yang, T.M. Lavaute, X. J. Li, M. Ayala, G.I. Bondarenko, Z.W. Du, Y. Jin, T.G. Golos, S.C. Zhang, Pax6 is a human neuroectoderm cell fate determinant, Cell Stem Cell 7 (1) (2010) 90–100.
[35] U. Lendahl, L.B. Zimmerman, R.D. McKay, CNS stem cells express a new class of intermediate filament protein, Cell 60 (4) (1990) 585–595.
[36] B.G. Herrmann, A. Kispert, The T genes in embryogenesis, Trends Genet. 10 (8) (1994) 280–286.
[37] Y. Saga, S. Kitajima, S. Miyagawa-Tomita, Mesp1 expression is the earliest sign of cardiovascular development, Trends Cardiovasc. Med. 10 (8) (2000) 345–352.
[38] G. Bazzoni, P. Tonetti, L. Manzi, M.R. Cera, G. Balconi, E. Dejana, Expression of junctional adhesion molecule-a prevents spontaneous and random motility, J. Cell Sci. 118 (Pt 3) (2005) 623–632.

[39] J. Munoz, T.Y. Low, Y.J. Kok, A. Chin, C.K. Frese, V. Ding, A. Choo, A.J. Heck, The quantitative proteomes of human-induced pluripotent stem cells and embryonic stem cells, Mol. Syst. Biol. 7 (2011) 550.
[40] J.M. Ramirez, S. Gerbal-Chaloin, O. Milhavet, B. Qiang, F. Becker, S. Assou, J. M. Lemaitre, S. Hamamah, J. De Vos, Brief report: benchmarking human pluripotent stem cell markers during differentiation into the three germ layers unveils a striking heterogeneity: all markers are not equal, Stem Cells 29 (9) (2011) 1469–1474.
[41] P. Madrigal, S. Deng, Y. Feng, S. Militi, K.J. Goh, R. Nibhani, R. Grandy, A. Osnato, D. Ortmann, S. Brown, S. Pauklin, Epigenetic and transcriptional regulations prime cell fate before division during human pluripotent stem cell differentiation, Nat. Commun. 14 (1) (2023) 405.
[42] J. Zhang, I. Khvorostov, J.S. Hong, Y. Oktay, L. Vergnes, E. Nuebel, P.N. Wahjudi, K. Setoguchi, G. Wang, A. Do, H.J. Jung, J.M. McCaffery, I.J. Kurland, K. Reue, W. N. Lee, C.M. Koehler, M.A. Teitell, UCP2 regulates energy metabolism and differentiation potential of human pluripotent stem cells, EMBO J. 30 (24) (2011) 4860–4873.
[43] A. Novak, M. Amit, T. Ziv, H. Segev, B. Fishman, A. Admon, J. Itskovitz-Eldor, Proteomics profiling of human embryonic stem cells in the early differentiation stage, Stem Cell Rev. Rep. 8 (1) (2012) 137–149.
[44] S. Mostafavi, N. Balafkan, I.K.N. Pettersen, G.S. Nido, R. Siller, C. Tzoulis, G. J. Sullivan, L.A. Bindoff, Distinct mitochondrial Remodeling during mesoderm differentiation in a human-based stem cell model, Front. Cell Dev. Biol. 9 (2021) 744777.
[45] M.J. Evans, M.H. Kaufman, Establishment in culture of pluripotential cells from mouse embryos, Nature 292 (5819) (1981) 154–156.
[46] Y. Sugano, M. Takeuchi, A. Hirata, H. Matsushita, T. Kitamura, M. Tanaka, A. Miyajima, Junctional adhesion molecule-a, JAM-A, is a novel cell-surface marker for long-term repopulating hematopoietic stem cells, Blood 111 (3) (2008) 1167–1172.
[47] K.R. Boheler, S. Bhattacharya, E.M. Kropp, S. Chuppa, D.R. Riordon, D. Bausch-Fluck, P.W. Burridge, J.C. Wu, R.P. Wersto, G.C. Chan, S. Rao, B. Wollscheid, R. L. Gundry, A human pluripotent stem cell surface N-glycoproteome resource reveals markers, extracellular epitopes, and drug targets, Stem Cell Rep. 3 (1) (2014) 185–203.
[48] J.L. Toran, J.A. Lopez, P. Gomes-Alves, S. Aguilar, C. Torroja, M. Trevisan-Herraz, I. Moscoso, M.J. Sebastiao, M. Serra, C. Brito, F.M. Cruz, J.C. Sepulveda, J.L. Abad, C. Galan-Arriola, B. Ibanez, F. Martinez, M.E. Fernandez, F. Fernandez-Aviles, I. Palacios, R.B. L, J. Vazquez, P.M. Alves, A. Bernad, Definition of a cell surface signature for human cardiac progenitor cells after comprehensive comparative transcriptomic and proteomic characterization, Sci. Rep. 9 (1) (2019) 4647.
[49] V.Y. Ng, S.N. Ang, J.X. Chan, A.B. Choo, Characterization of epithelial cell adhesion molecule as a surface marker on undifferentiated human embryonic stem cells, Stem Cells 28 (1) (2010) 29–35.
[50] S. Stelzer, K. Ebnet, J.C. Schwamborn, JAM-A is a novel surface marker for NG2-glia in the adult mouse brain, BMC Neurosci. 11 (2010) 27.
[51] A.G. Solimando, A. Brandl, K. Mattenheimer, C. Graf, M. Ritz, A. Ruckdeschel, T. Stuhmer, Z. Mokhtari, M. Rudelius, J. Dotterweich, M. Bittrich, V. Desantis, R. Ebert, P. Trerotoli, M.A. Frassanito, A. Rosenwald, A. Vacca, H. Einsele, F. Jakob, A. Beilhack, JAM-A as a prognostic factor and new therapeutic target in multiple myeloma, Leukemia 32 (3) (2018) 736–743.
[52] A.M. Rosager, M.D. Sorensen, R.H. Dahlrot, H.B. Boldt, S. Hansen, J.D. Lathia, B. W. Kristensen, Expression and prognostic value of JAM-A in gliomas, J. Neuro-Oncol. 135 (1) (2017) 107–117.
[53] N.B. Ivanova, J.T. Dimos, C. Schaniel, J.A. Hackney, K.A. Moore, I.R. Lemischka, A stem cell molecular signature, Science 298 (5593) (2002) 601–604.
[54] T. Sakaguchi, M. Nishimoto, S. Miyagi, A. Iwama, Y. Morita, N. Iwamori, H. Nakauchi, H. Kiyonari, M. Muramatsu, A. Okuda, Putative “stemness” gene jam-B is not required for maintenance of stem cell state in embryonic, neural, or hematopoietic stem cells, Mol. Cell. Biol. 26 (17) (2006) 6557–6570.
[55] M.R. Cera, A. Del Prete, A. Vecchi, M. Corada, I. Martin-Padura, T. Motoike, P. Tonetti, G. Bazzoni, W. Vermi, F. Gentili, S. Bernasconi, T.N. Sato, A. Mantovani, E. Dejana, Increased DC trafficking to lymph nodes and contact hypersensitivity in junctional adhesion molecule-A–deficient mice, J. Clin. Invest. 114 (5) (2004) 729–738.
[56] G. Gliki, K. Ebnet, M. Aurrand-Lions, B.A. Imhof, R.H. Adams, Spermatid differentiation requires the assembly of a cell polarity complex downstream of junctional adhesion molecule-C, Nature 431 (7006) (2004) 320–324.